

The influence of charge and flexibility on smectic phase formation in filamentous virus suspensions

Kirstin Purdy and Seth Fraden

*Complex Fluids Group, Martin Fisher School of Physics,
Brandeis University, Waltham, Massachusetts 02454*

(Dated: March 23, 2019)

Abstract

We present experimental measurements of the cholesteric-smectic phase transitions of suspensions of charged semiflexible rods as a function of rod flexibility and surface charge. The rod particles are structurally identical to M13 virus but vary in either contour length, and therefore ratio of persistence length to contour length, or surface charge. Surface charge is altered by changing solution pH and by comparing M13 to *fd* virus, which differs from M13 only by the substitution of a single charged amino acid for a neutral one per viral coat protein. Phase diagrams are measured as a function of particle length, particle charge and ionic strength. The experimental results are compared with existing theoretical predictions for the phase behavior of flexible rods and charged rods. In contrast to the isotropic-cholesteric transition, where theory and experiment agree, the nematic-smectic transition exhibits complex charge and ionic strength dependence not predicted by theory. Possible explanations for these unexpected electrostatic interactions are discussed.

INTRODUCTION

In a suspension of hard or charged rods, purely repulsive entropic interactions are sufficient to induce liquid crystal ordering. Theoretically, hard rods exhibit isotropic, nematic and smectic phases with increasing concentration [1, 2, 3]. Unfortunately, although theoretically simple objects, production of hard, rigid monodisperse rods is very difficult. Rigid and flexible polyelectrolyte rods, however, are abundant, especially in biological systems, which by nature lend themselves to mass-production. Viruses, such as *fd*, M13 and Tobacco Mosaic Virus (TMV) are a unique choice for use in studying liquid crystal phase behavior, in that they are biologically produced to be monodisperse and are easily modified by genetic engineering and post-expression chemical modification. These virus particles are also, to our knowledge, the only colloidal systems known to exhibit the predicted hard-rod phase progression (isotropic-nematic-smectic) [4, 5]. Suspensions of charged β -FeOOH rods [6] are the only other system known to form a stable smectic phase. Accurately describing the nematic-smectic (N-S) transition for charged and/or flexible rods is important because it elucidates the nature of interparticle interactions. Even though qualitative theories have been developed to describe the effects of electrostatics *or* flexibility on the N-S phase boundary [7, 8, 9], many challenges remain to correctly describe this transition for charged *and* flexible particles. Near the N-S transition, the particles are at very high concentrations, and as we will show, dilute-limit approximations of interparticle interactions which are appropriate at the isotropic-nematic transition cannot be used. Additionally, our results add insight into the ordering of other important rodlike polyelectrolytes including biopolymers like DNA and F-actin.

In this paper we will test the limits of current theoretical predictions for the nematic-smectic phase transition in two ways. First, we measure the ionic strength dependence of the phase transition for filamentous virus of identical structure and varied length. By changing the rod length and leaving local particle structure constant, the rod flexibility is altered as defined by the ratio of persistence length P , or half the Kuhn length, to contour length L , or P/L . In our experiments the flexibility of the particles remains within the semiflexible limit, meaning $P \sim L$. Altering the particle flexibility probes the competition between rigid and

flexible rod phase behavior in the semiflexible limit. It also allows us to probe the efficacy of current methods for incorporating electrostatic repulsion into hard-particle theories through measurements of a large number of values of ionic strength and particle size. Second, we measure the nematic-smectic phase transition for filamentous virus of different charge. Altering the surface charge by two independent techniques, solution chemistry and surface chemistry, probes the importance of the details of the surface charge distribution in determining long range interparticle interactions. By varying these three independent variables, length, charge and solution ionic strength, we systematically determine how electrostatic interactions and flexibility experimentally effect the nematic-smectic phase boundary.

For our colloidal rods we use the rodlike semiflexible bacteriophages *fd* and M13. In solution, these virus particles form isotropic (I), cholesteric (nematic) and smectic (S) phases with increasing concentration [8, 10, 11, 12]. We note that the free energy difference between the cholesteric and nematic (N) phases is small, and therefore it is appropriate to compare our results with predictions for the nematic phase. M13 and *fd* differ from one another by only one amino acid per coat protein; the negatively charged aspartate (asp₁₂) in *fd* is substituted for the neutral asparagine (asn₁₂) in M13 [13], and thus are ideal for use in studying charge dependence of phase behavior. Changes in the surface charge of the particles were also achieved by varying the pH of the solution [14]. By varying the length of the M13 DNA we created M13 mutants which differ only in contour length. The M13 mutants have the same local structure, and thus we assume persistence length, as M13. These mutant M13 viruses were used to measure the flexibility dependence of the nematic-smectic phase transition.

MATERIALS AND METHODS

Properties of *fd* and M13 include length $L = 0.88\mu\text{m}$, diameter $D = 6.6\text{nm}$, and persistence length $P = 2.2\mu\text{m}$ [5]. The M13 mutants have lengths of $1.2\mu\text{m}$, $0.64\mu\text{m}$, and $0.39\mu\text{m}$ [12]. Virus production is explained elsewhere [15]. Two of the length-mutants ($0.64\mu\text{m}$ and $0.39\mu\text{m}$) were grown using the phagemid method [12, 15] which produces bidisperse solutions of the phagemid and the $1.2\mu\text{m}$ helper phage. Sample polydispersity was checked using gel

electrophoresis on the intact virus, and on the viral DNA. Excepting the phagemid solutions which were 20% by mass 1.2 μm helper phage, virus solutions were highly monodisperse as indicated by sharp electrophoresis bands. The bidispersity in the phagemid solution does not suppress smectic phase formation [12].

All samples were dialyzed against a 20mM Tris-HCl buffer at pH 8.2 or 20 mM Sodium Acetate buffer adjusted with Acetic Acid to pH 5.2. To vary ionic strength, NaCl was added to the buffering solution. The linear surface charge density of *fd* is approximately 10 e^-/nm at pH 8.2 and 7 e^-/nm at pH 5.2 [14]. M13 surface charge was calculated from the known *fd* surface charge by comparing both molecular composition and electrophoretic mobilities [16]. As M13 and *fd* are identical accept for their surface charge, their electrophoretic mobility difference is proportional to their net surface charge difference [17]. By multiplying the known *fd* charge by the ratio of M13 and *fd* electrophoretic migration (*fd* migrates 200% faster than M13 at pH 5.2 and 150% faster at pH 8.2), we find that the linear surface charge density of M13 is approximately 7 e^-/nm at pH 8.2 and 3.6 e^-/nm at pH 5.2, in agreement with calculations from molecular composition.

After dialysis, the virus suspensions were concentrated via ultracentrifugation at 200 000 g and diluted to concentrations just above the N-S transition. Since knowing the surface charge of the virus is critical to our analysis of the N-S transition, we experimentally measured the pH of the virus solutions at concentrations in the nematic phase just below the N-S transition. We found that for an initial buffer solution at pH 8.2 (Tris-HCl buffer $\text{pKa}=8.2$), the pH of the concentrated virus suspensions is slightly less than 8.2, but still well within the buffering pH range ($\text{pH}=\text{pKa}\pm1$). The surface charge does not change significantly over this range [14]. At pH 5.2 (Acetic acid buffer $\text{pKa}=4.76$) the measured pH of the virus suspensions near the N-S transition was slightly higher than 5.2. This shift further away from the pKa may effect the buffering ability of the solution and subsequently the phase behavior. Additionally, the shift in pH becomes stronger with decreasing ionic strength, most likely due to the relatively high concentration of virus counterions (50-100 mM) as compared to buffer ions (20 mM). The implications of these measurements are discussed further in the Results section.

All measurements were done at room temperature. The concentration of the phases was measured by absorption spectrophotometry with the optical density (A) of the virus being $A_{269\text{nm}}^{1\text{mg/ml}} = 3.84$ for a path length of 1 cm.

ELECTROSTATIC INTERACTIONS

The total rod-rod interparticle interaction includes a combination of hard core repulsion and long ranged electrostatic repulsion. We present two possible ways to incorporate the electrostatic repulsion into hard-rod theories. First, it is possible to define an effective hard core diameter (D_{eff}) larger than the bare diameter D , which is calculated from the second virial coefficient of the free energy for charged rods [1, 18]. Increasing ionic strength decreases D_{eff} , but for highly charged colloids, like M13 and *fd*, the effect of surface charge on D_{eff} is small as the non-linear nature of the Poisson-Boltzmann equation leads to counterion condensation near the colloid surface which renormalizes the bare surface charge to a lesser effective charge, which is nearly independent of the bare surface charge [11, 19]. It has been experimentally verified that this effective diameter accurately describes the electrostatic repulsion between virus particles at the isotropic- nematic (I-N) transition in the limit of large L/D_{eff} [11, 16]. Previously, we showed that a D_{eff} independent of virus concentration could describe the electrostatic interactions of virus suspensions at the nematic-smectic transition [8]. However, we note that the use of D_{eff} beyond the regime where the second virial coefficient quantitatively describes the system (above the isotropic-nematic transition) is not necessarily justified. We show in this paper that this crude treatment of the electrostatic interactions neglects significant features predicted by the scaled particle theory described in the following paragraph.

An alternative effective diameter was developed by Kramer and Herzfeld. They calculate an “avoidance diameter” D_a which minimizes the scaled particle expression for the free energy of charged parallel spherocylinders as a function of concentration[7]. With respect to ionic strength, D_a exhibits the same trend as D_{eff} , but is defined to be independent of charge within the “highly charged” colloid regime. Specifically, the renormalized surface charge of the colloidal rods in Kramer and Herzfeld’s theory is defined to be $1\text{ e}^-/7.1\text{ \AA}$ for any colloidal

rod (including *fd* and M13) with a surface charge greater than or equal to $1 \text{ e}^-/7.1 \text{ \AA}$ [7]. The advantage of this theory over Onsager's effective diameter is its use of scaled particle theory. By using the scaled particle theory, third and higher virial coefficients are accounted for in an approximate way [20, 21], making this “avoidance diameter” more appropriate for incorporating electrostatic interactions at the nematic-smectic transition. The disadvantage is that the free energy expression developed by Kramer [7] does not reduce to Onsager's theory in the absence of no electrostatic interactions. Kramer's calculations [7] qualitatively reproduce previously published data for the N-S transition of *fd* virus, but the limited range of data previously available did not include some of the interesting features described in this theory, which we are now able to test. Having an appropriate way to describe the electrostatic interactions between rods is essential for separating the effects of charge, ionic strength and flexibility on the N-S phase behavior we now present.

RESULTS

The location of the N-S transition was determined by measuring the highest nematic concentration (ϕ^N) and the lowest smectic concentrations (ϕ^S) observed, with $\phi = \pi LD^2 c/4$ and c equal to the nematic or smectic rod number density respectively. Because of the high viscosity of the suspensions near the N-S transition, bulk separation of the nematic and smectic phases is not observed, however, smectic or nematic domains can be observed using differential interference contrast microscopy (DIC) in coexistence with predominantly nematic and smectic bulk phases, respectively. Typically coexistence is observed as ribbons of smectic phase reaching into a nematic region.

Measurements of ϕ^S are presented in Fig. 1 as a function of the M13 mutant particle length, and therefore virus flexibility by L/P , for multiple ionic strengths. The influence of flexibility on the nematic-smectic transition of hard-rods has been well studied theoretically [9, 22]. Adding a small amount of flexibility is expected to drive the smectic phase to higher concentrations, from the predicted hard-rigid-rod concentration of $\phi^S=0.47$ [2], to approximately $0.75 \lesssim \phi^S \lesssim 0.8$ within the semiflexible limit [9]. Once within the semiflexible limit, however, ϕ^S is essentially independent of flexibility. At a constant ionic strength Fig.

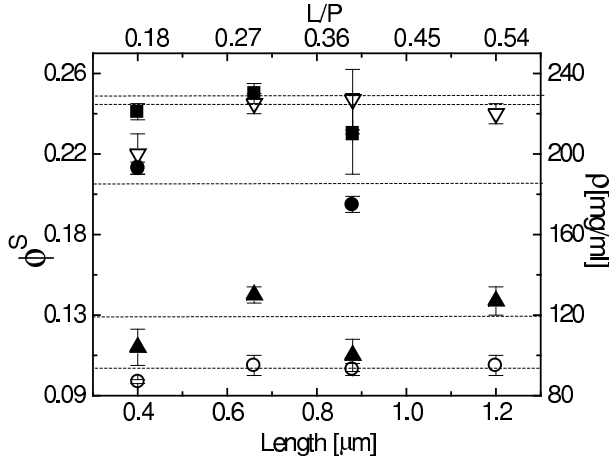


FIG. 1: Smectic phase concentration ϕ^S at the N-S transition for multiple ionic strengths at pH 8.2 as a function of rod length L and flexibility L/P . Legend for ionic strengths is as follows: \circ 5 mM, \blacktriangle 10 mM, \bullet 60 mM, \bigtriangledown 110 mM, \blacksquare 150 mM. With increasing ionic strength ϕ^S increases due to increasing electrostatic screening. Dashed lines are a guide to the eye at constant ionic strength. Within experimental accuracy the smectic phase transition is independent of flexibility within the range $0.18 < L/P < 0.54$.

1 shows that within experimental accuracy ϕ^S is independent of virus length, and thus independent of changing flexibility in the range of $0.18 < L/P < 0.24$, as predicted. This is in striking contrast to the significant flexibility dependence measured at isotropic-nematic transition for this same system of semiflexible M13 mutants which is described in [16]. At the isotropic-nematic transition the dimensionless concentration $bc = \phi^{I-N}L/D$ increases with increasing flexibility in agreement with theoretical predictions by Khokhlov and Semenov [23, 24], especially at high ionic strength where L/D_{eff} is large.

As seen in Fig. 1, ionic strength plays an important role in determining the phase boundaries by screening electrostatic interactions. To compare our charged-flexible-rod results with predictions for the N-S phase transition of hard (rigid or flexible) rods, we graph in Fig. 2 ϕ_{eff}^N as a function of rod length. We define $\phi_{\text{eff}}^N = \phi^N(D_{\text{eff}}^N)^2/D^2$. Because crossed charged rods have a lower energy than parallel charged rods D_{eff}^N increases with particle alignment reaching a maximum possible value of $D_{\text{eff}}^N = 1.12D_{\text{eff}}^{\text{iso}}$, just below the smectic phase, with $D_{\text{eff}}^{\text{iso}}$ equal to the isotropic effective diameter [8, 18]. The effective volume fraction ϕ_{eff}^N should be equivalent to the hard-flexible rod concentration and be independent of ionic strength if D_{eff}^N

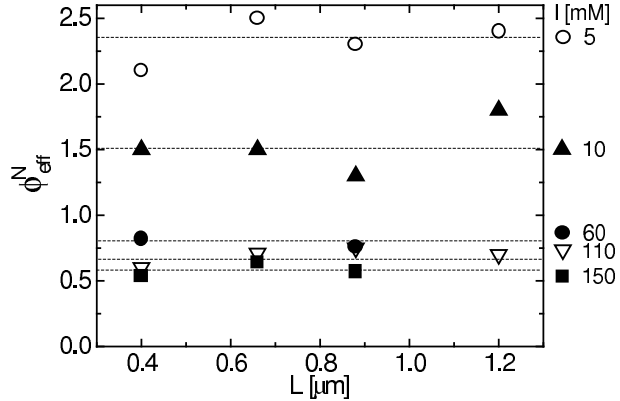


FIG. 2: Nematic phase effective volume fraction ϕ_{eff}^N at the N-S transition for multiple ionic strengths at pH 8.2 as a function of L . Legend for symbols is to the right of the figure. Dashed lines drawn are a guide to the eye and are at constant ionic strength. Because ϕ_{eff}^N strongly depends on ionic strength, we conclude that D_{eff}^N does not describe the electrostatic interactions at high virus concentrations.

accurately models the interparticle electrostatic interactions. However, ϕ_{eff}^N depends quite strongly on ionic strength in Fig. 2. Previously, we observed $\phi_{\text{eff}}^N = 0.75$ independent of ionic strength for suspensions of *fd* virus [8]. Though our data agrees semi-quantitatively with this near $I=60$ mM, by expanding our measurements to include larger values ionic strength as well as multiple particle lengths, we clearly measure an ionic strength dependence in ϕ_{eff}^N with ϕ_{eff}^N ranging from 2.5 to 0.5. This large ionic strength dependence of ϕ_{eff}^N indicates that D_{eff}^N is not sufficient for describing the electrostatic interactions at the N-S transition. This is not entirely surprising due to the fact that D_{eff} is strictly defined to be accurate at low concentrations where two-particle interactions are dominant.

We show in Fig. 3 the volume fraction of the nematic-smectic transition, ϕ^N and ϕ^S averaged over results from all particle lengths as a function of ionic strength. With increasing ionic strength the electrostatic repulsion between rods decreases approaching hard-rod phase behavior in the limit of very high ionic strength. We observe that above approximately $I=100$ mM, ϕ^S becomes independent ionic strength due to a effective “close packing” of the rods in the smectic phase. This saturation at high ionic strength is consistent with the phase behavior predicted by Kramer for parallel charged spherocylinders with a concentration dependent avoidance diameter D_a , as mentioned previously [7]. However, Kramer’s theory

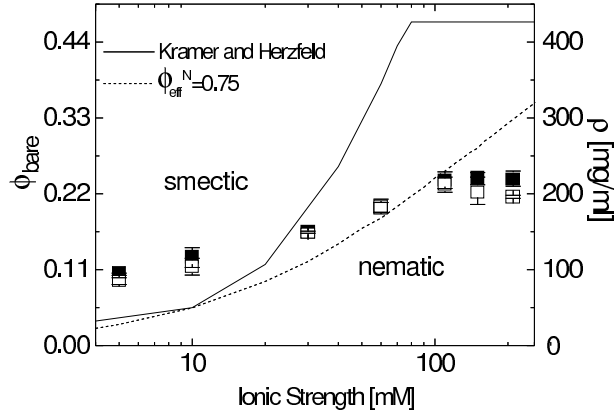


FIG. 3: Average concentration of the nematic (open) and smectic (solid) phases at the N-S transition as a function of ionic strength at pH 8.2. Average is over the four M13 length mutants. Solid line is taken from simulations by Kramer and Herzfeld [7] for particles the same size as *fd* and with a renormalized surface charge of $1e^-/7.1$ Å. Dashed line is $\phi_{\text{bare}} = \phi_{\text{eff}}^N * D^2 / (D_{\text{eff}}^N)^2$ with $\phi_{\text{eff}}^N = 0.75$.

predicts a saturation concentration of $\phi_{\text{sat}}^S = 0.47$, or the theoretical hard-spherocylinder ($I \rightarrow \infty$) limit [2, 7], which is much higher than our experimental saturation value of $\phi_{\text{sat}}^S = 0.24$. This discrepancy is most likely due to the role of electrostatics being much stronger than predicted by D_a , as flexibility, our other independent variable, is predicted to increase, not decrease, the N-S transition concentration. Contrastingly, simply scaling ϕ^N by D_{eff}^2 , does not capture this sudden saturation, as shown by the dashed curve for $\phi_{\text{eff}}^N = 0.75$, in Fig. 3. Both approximations for the electrostatic interactions qualitatively reproduce some features of the N-S transition yet they both differ significantly from the experimentally observed behavior.

In addition to measuring the effect of ionic strength on the phase behavior, we also measured the effect rod surface charge. We measure the phase behavior of *fd* and M13 at pH 5.2 and pH 8.2. Fig. 4 presents the ionic strength and pH dependence of the N-S phase transition for *fd* (a) and M13 (b). Similar to the trend in Fig. 3, increasing ionic strength increases the N-S transition concentration, until about 100 mM ionic strength, above which ϕ^S is independent of ionic strength. Above about 100 mM, the *fd* phase boundary saturates around $\phi_{\text{sat}}^S \sim 0.21$, independent of pH, and the M13 phase boundary saturates around $\phi_{\text{sat}}^S = 0.24$, also independent of pH. Surprisingly, at these high ionic strengths, where the

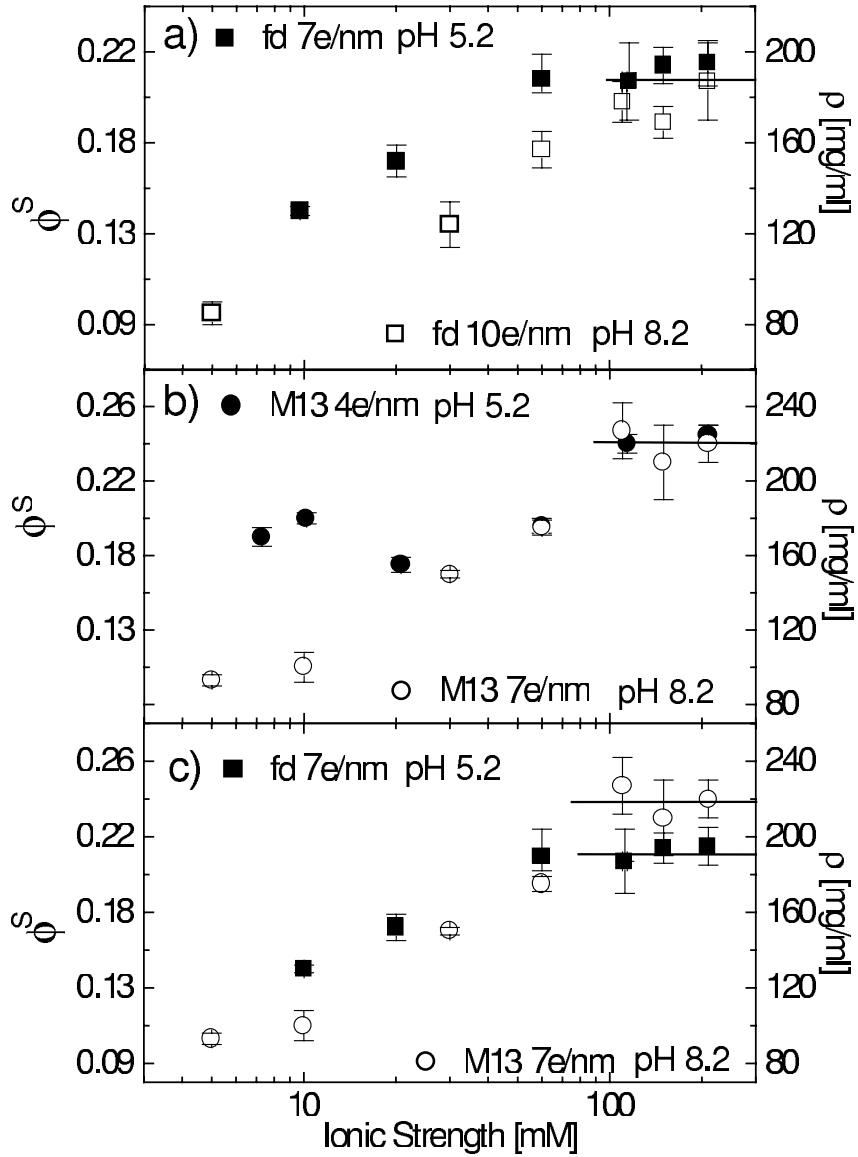


FIG. 4: Nematic-smectic phase transition concentration as function of ionic strength for suspensions of a) *fd* and b) M13 at pH 5.2 (solid) and pH 8.2 (open). Figure c) shows M13 (pH 8.2) and *fd* (pH 5.2) at 7 e/nm surface charge. Solid lines highlight the ionic strength independence at high ionic strength.

surface charge should be well screened, *fd* suspensions have a phase boundary at lower concentrations than the M13 suspensions, independent of pH.

At low ionic strength, below about 100 mM, the pH dependence of the N-S transition is stronger than at high ionic strength, as shown in Fig. 4a,b. Suspensions at higher pH (higher surface charge) consistently enter a smectic phase at lower concentrations. This is

surprising because at the isotropic-nematic transition, where the charge dependence is well described by D_{eff} , the surface charge dependence of the phase transition is very small [16]. Additionally, the non-linearity of the Poisson-Boltzmann equation predicts that the long-range electrostatic potential between rods is insensitive to surface charge changes and thus pH changes [1, 18]. The high sensitivity of the N-S transition to changes in pH indicates that the charge independent nature of both D_{eff} and D_a does not correctly characterize the electrostatic interactions at the N-S transition.

It is also unexpected that M13 and *fd* would have different phase behavior even when both virus have the same predicted surface charge of $7\text{e}^-/\text{nm}$, as shown in Fig. 3c. At low ionic strength the phase behavior is similar, but *fd* suspensions consistently enter the smectic phase at a slightly higher concentration. At high ionic strength, the reverse is true; *fd* has a lower phase transition concentration than M13 suspensions, as mentioned above. At low ionic strength, the slight difference in phase transition concentrations between M13 at pH 8.2 and *fd* at pH 5.2 could be due to the measured increase in pH at low ionic strength and low pH. Shifts in the pH, particularly near the viral pKa ($\text{pKa}_{fd} = 4$), i.e. at pH 5.2, can shift the viral surface charge. Because the measured pH is higher than the original buffer, the actual surface charge of the *fd* particles at pH 5.2 may have increased slightly. A small increase in the surface charge of the *fd* samples would account for the disagreement with the M13 measurements. We stress however, that this high sensitivity of the N-S transition to surface charge differences, is not predicted by either D_{eff} or D_a .

The difference between M13 and *fd* saturation concentrations at high ionic strength and equal surface charge (Fig. 4c), however, is not well explained by this argument. At high ionic strength, the measured pH of the concentrated virus solutions is not significantly different from the initial buffer pH, as mentioned in the Materials and Methods. However, at high ionic strength ($I > 110 \text{ mM}$) adjacent virus surfaces are separated by distances smaller than the virus diameter (6.6 nm) [26], which is on the order of the spacing between viral coat-proteins (1.6 nm) and the Debye screening length $\kappa = 3.0 \text{ \AA}/\sqrt{I} = 0.9 \text{ nm}$. Because the rods are separated by distances on the order of the Debye screening length, the actual surface charge configuration of the viral rods can no longer be approximated as a continuous charge

distribution as is done in the effective diameter calculation. Furthermore, it has been shown theoretically that discretization of the surface charges can change the predicted counterion condensation when compared to the non-linear Poisson Boltzmann equation [27]. Perhaps it is because we are in the regime where the surface charge configuration can no longer be neglected that we observe charge-configuration-dependent saturation of the nematic-smectic phase transition. Theoretical models or simulations of the electrostatic interactions of a dense, rod-like polyelectrolyte system, which include the detail of the surface charge configuration may shed light on the experimental differences between M13 and *fd* nematic-smectic transitions at high ionic strength.

CONCLUSION

In summary, we have presented the nematic-smectic phase diagram as a function of length, surface charge and ionic strength. We observed that in the semiflexible-rod limit the N-S phase boundary is independent of rod flexibility in contrast to the strong flexibility dependence seen at the isotropic-nematic transition. By studying the ionic strength dependence of this transition we observed that renormalizing ϕ^S by Onsager's effective diameter does not produce an ionic-strength independent phase transition concentration, which would be necessary to compare the flexible-rod phase behavior to hard-particle theories. Scaled particle theory and Kramer and Herzfeld's avoidance diameter qualitatively reproduce the observed N-S phase behavior, but more theoretical work is needed to find a way to compare the charged-flexible rod results to the hard-flexible rod theories available. Furthermore, significant differences were measured between M13 and *fd* N-S phase behavior, even when they shared the same surface charge. These results indicate that the electrostatic interactions between these rods are much more complicated than can be accounted for by calculating the interparticle potential assuming a uniform renormalized surface charge. We hypothesized that the electrostatic interactions between rods could be influenced by the configuration of the charged amino acids on the rod surface. Experimental confirmation of this could be found by measuring M13 and *fd* equations of state (pressure vs density), and thus the particle-particle interactions, as a function of solution salt and pH, as in techniques devel-

oped for DNA [28].

We acknowledge support from the NSF(DMR-0088008).

- [1] L. Onsager, Ann. NY Acad. Sci. **51**, 627 (1949).
- [2] P. G. Bolhuis and D. Frenkel, J. Chem. Phys. **106**, 668 (1997).
- [3] J. M. Polson, Phys. Rev. E **56**, R6260 (1997).
- [4] R. B. Meyer, in *Dynamics and Patterns in Complex Fluids*, edited by A. Onuki and K. Kawasaki (Springer-Verlag, 1990), p. 62.
- [5] S. Fraden, in *Observation, Prediction, and Simulation of Phase Transitions in Complex Fluids*, edited by M. Baus, L. F. Rull, and J. P. Ryckaert (Kluwer Academic, Dordrecht, 1995), pp. 113–164.
- [6] H. Maeda and Y. Maeda, Phys. Rev. Lett. **90**, 018303 (2003).
- [7] E. M. Kramer and J. Herzfeld, Phys. Rev. E **61**, 6872 (2000).
- [8] Z. Dogic and S. Fraden, Phys. Rev. Lett. **78**, 2417 (1997).
- [9] A. V. Tkachenko, Phys. Rev. Lett. **77**, 4218 (1996).
- [10] J. Lapointe and D. A. Marvin, Mol. Cryst. Liq. Cryst. **19**, 269 (1973).
- [11] J. Tang and S. Fraden, Liquid Crystals **19**, 459 (1995).
- [12] Z. Dogic and S. Fraden, Phil. Trans. R. Soc. Lond. A. **359**, 997 (2001).
- [13] D. A. Marvin, R. D. Hale, C. Nave, and M. H. Citterich, J. Molec. Bio. **235**, 260 (1994).
- [14] K. Zimmermann, J. Hagedorn, C. C. Heuck, M. Hinrichsen, and J. Ludwig, J. Biol. Chem. **261**, 1653 (1986).
- [15] J. Sambrook, E. F. Fritsch, and T. Maniatis, in *Molecular Cloning: A Laboratory Manual* (Cold Spring Harbor Laboratory, New York, 1989), chap. 4, 2nd ed.
- [16] K. R. Purdy and S. Fraden, unpublished.
- [17] J. T. G. Overbeek, in *Advances in Colloid Science*, edited by H. Mark and E. J. W. Verwey (Interscience Publishers, New York, 1950), pp. 97–135.
- [18] A. Stroobants, H. N. W. Lekkerkerker, and D. Frenkel, Phys. Rev. Lett. **57**, 1452 (1986).

- [19] G. S. Manning, J. Chem. Phys. **51**, 924 (1969).
- [20] M. A. Cotter and D. C. Wacker, Phys. Rev. A **18**, 2669 (1978).
- [21] M. A. Cotter, in *The Molecular Physics of Liquid Crystals*, edited by G. R. Luckhurst and G. W. Gray (Academic Press, London, 1979), pp. 169–189.
- [22] P. van der Schoot, J. Phys. II France **6**, 1557 (1996).
- [23] A. R. Khokhlov and A. N. Semenov, Physica A **112**, 605 (1982).
- [24] Z. Y. Chen, Macromolecules **26**, 3419 (1993).
- [25] K. Dogic, Ph.D. thesis, Brandeis University (2004).
- [26] K. R. Purdy, Z. Dogic, S. Fraden, A. Rühm, L. Lurio, and S. G. J. Mochrie, Phys. Rev. E **67**, 031708 (2003).
- [27] M. L. Henle, C. D. Santangelo, D. M. Patel, and P. A. Pincus, Europhys. Lett. **66**, 284 (2004).
- [28] H. H. Strey, V. A. Parsegian, and R. Podgornik, Phys. Rev. Lett. **78**, 895 (1997).